

PARAMETER IDENTIFICATION OF FLUID VISCOUS DAMPERS

***Rita GRECO¹ and Giuseppe Carlo MARANO²**

¹ DICATECH, Department of Civil Engineering, Environmental, Territory, Building and Chemical, Technical University of Bari, via Orabona 4 - 70125, Bari -Italy.

² DICAR, Department of civil Engineering and Architecture, Technical University of Bari, via Orabona 4 - 70125, Bari -Italy

*Corresponding author: rita.greco@poliba.it

This paper focuses on parameter identification of Fluid Viscous Dampers, comparing different existing literature models, with the aim to recognize ability of these models to match experimental loops under different test specimens. Identification scheme is developed evaluating the experimental and the analytical values of the forces experienced by the device under investigation. The experimental force is recorded during the dynamic test, while the analytical one is obtained by applying a displacement time history to the candidate mechanical law.

Identification procedure furnishes device mechanical parameters by minimizing a suitable objective function, which represents a measure of difference between analytical and experimental forces. To solve optimization problem, the Particle Swarm Optimization is adopted, and the results obtained under various test conditions are shown. Some considerations about the agreement of different models with experimental data are furnished, and the sensitivity of identified parameters of analyzed models against frequency excitation is evaluated and discussed..

Keywords: Fluid Viscous Damper, parameters identification, Kelvin-Voigt model, Particle Swarm Optimization

Introduction

In recent years, several devices have been proposed to reduce the effects of dynamic loads in civil structures and infrastructures. In this paper, the attention is focused on Fluid Viscous Dampers (FVD), generally viewed as passive dissipation elements [1], widely adopted in many civil engineering applications to reduce the vibration level and to increase structural protection level against wind and earthquake forces (see for instance [2],[3]). Among the most interesting features of viscous dampers, one should mention low maintenance costs, usability for several earthquakes without damage and viscous forces out-of-phase with the elastic ones.

Viscous dampers utilized in civil structures to control seismic, wind induced and thermal expansion motions, are usually arranged in one of the following configurations: a diagonal or chevron bracing element within a steel or concrete frame, as a part of the cable stays of long-span bridges, as a part of tuned mass dampers, as a part of a base isolation system to increase the energy dissipation and as a device to allow free thermal movements [4]. Viscous dampers can be efficiently used in the construction of new buildings or in retrofitting existing structures. The importance of viscous dampers in vibration control has increased thanks to their energy dissipation capability and wide range of applications.

A viscous fluid damper typically consists [1] of a piston within a damper housing, filled with a compound of silicone or similar type of oil. The fluid passes through several small orifices from one side of the piston to the other; therefore, the energy is dissipated through the concept of fluid orificing. The fluid damper produces a force that is not always proportional to velocity [5], depending on the type of orifice used. The orifice utilizes a series of passages to alter flow characteristics with fluid speed. The "fluid control orifice" provides forces proportional to v^α , where α is a coefficient varying in the range $[0.5 \div 1]$. When $\alpha=1$, the behavior of FVD is linear and in earthquake engineering applications this is the most desired circumstance. Actually, FVDs contain valves instead of the piston within orifices. These valves are opened once the transmitted force exceeds a certain design limit. However, the force produced by FVD is not proportional to velocity, and also in this case the valves provide forces proportional to v^α .

Since the applications of viscous dampers are growing very fast, the exact recognition of their mechanical behavior is of primary importance to provide a reliable support to design an efficient seismic protection strategy. Current identification techniques for viscous dampers are mostly based

on parametric models. Although parametric identification techniques have been successfully used to identify viscous dampers, non-parametric identification techniques are more suitable in structural health monitoring, because the system characteristics may continuously vary over time, both quantitatively as well as qualitatively.

Several identification approaches, both parametric and nonparametric, are compared in [4], by using real data carried out from full-scale nonlinear viscous dampers, commonly used in large flexible bridges. About the parametric techniques, the capability of the Adaptive Random Search is explored in [4]: the authors solved an optimization problem in which the numerical values of the unknown model parameters were estimated by minimizing an objective function based on the normalized mean square error between the measured and identified damper responses, evaluated as displacement/velocity, and obtained integrating dynamic equilibrium equations of FVD constitutive law, under experimental applied force history.

In this field, also soft-computing techniques, fuzzy inference systems and neural networks have been applied to model a Magneto Rheological Fluid Damper [6][7]. Evolutionary computation methods, e.g., Genetic Algorithms (GA) [8][9], have been widely applied in parameter identification applications and many others. Among different nonlinear models, especially the Bouc-Wen has been identified thanks to its versatility. In [10], the GA was employed to identify a mechatronic system of unknown structure. In this framework, a real-coded GA has been recently adopted in [11] to identify a piezoelectric actuator, whose hysteretic behavior has been modeled by the Bouc-Wen nonlinear law. A magneto-rheological fluid damper behavior has been recognized by [12], with reference to a non-symmetric version of the original Bouc-Wen model and by using a real coded GA. The final algorithm is very similar to the GA, but its efficiency has been improved in virtue of a selection procedure embedded into crossover and mutation genetic operators. The GA has been widely adopted to fit the Bouc-Wen model to hysteresis loops experimentally obtained for composite materials [13], non-linear degrading structures [14], magneto-rheological fluid dampers [15][16][17] or bolted-welded connections [18]. In [19], a new method based on GA is developed to identify the Bouc-Wen model parameters from experimental hysteretic loops, obtained from periodic loading tests.

Among evolutive algorithms, the Particle Swarm Optimization (PSO) [20] has been recognized as a promising candidate in parameter identification. The PSO is based on the multi-agent or population based philosophy (the particles) which mimics the social interaction in bird flocks or schools of fish, by incorporating the search experience of individual agents. Moreover, the PSO is effective in exploring the solution space in a relatively small number of iterations. PSO has been used in the design of PID controllers [21] and electro-magnetic [22]. The PSO convergence characteristic was analyzed in [23], where algorithm control settings were also proposed. In [24], a PSO algorithm is employed using experimental force-velocity data, obtained from various operating conditions, to identify the model parameters of a magneto rheological fluid damper.

In [25] a parameter identification for basic and generalized Kelvin-Voigt and Maxwell models for FVD is carried out. The identification procedure developed by means of particle swarm optimization gives the best mechanical parameters by minimizing a suitable objective function that represents a measure of difference between analytical and experimental applied forces. Results are obtained under various test conditions, comparing the agreement of various models with experimental data.

This paper focuses on parameter identification of FVD: the identification process is developed comparing the experimental and the analytical values of the forces experienced by the device under investigation. The experimental value of the force is recorded during the dynamic test, while the analytical one is obtained by applying the time history of displacements to the candidate mechanical law. In this way, a measure of the “distance” between experimental and analytical results is introduced, as the integral of the difference along the whole experiment. The optimal parameter set is thus derived by minimizing this distance using an evolutionary algorithm. For the parametric identification of FVD, the authors adopt an evolutive algorithm, the Particle Swarm Optimization. Different analytical models, characterized by increasing complexity, are considered and then are identified. The sensitivity against test conditions is also assessed.

The next of the paper is organized as follows: in section 2 there is a selection of models adopted in this study for FVD modeling; in section 3, the identification scheme is posed and in section 4, some remarks of PSO algorithm are given. Moreover, in section 5 some specifications of experimental tests are furnished; section 6 reports the results of identified parameters, which are discussed in section 7. Some conclusions are finally given in section 8.

MECHANICAL MODELS FOR FLUID-VISCOUS DAMPERS

System identification involves creating a model for a system that, with the same input as the original system, the model will produce an output that matches the original system output with a certain degree of accuracy. The input or excitation of the system and model, and their corresponding outputs, are used to create and tune the model until a satisfactory degree of accuracy is reached.

The application of non-classical methods for the parametric identification of viscous dampers requires: (i) the definition of an appropriate single-degree-of-freedom mechanical model and (ii) the formalization of the objective (or cost) function to be minimized. This section deals with the first aspect.

Generally, the system to be identified could be modeled by physical laws that reflect the dynamics of the system. A model created by laws, which reflect the physical properties of the system is called a white-box model. However, creating a white box model for real-world (complex) systems is a challenging task.

In structural applications, the selection of a proper model for FVD plays a central role to predict the real structural response after the identification. Generally, the description of FVD requires a suitable mechanical model, made of a set of springs and dashpots appropriately connected each other. In this study, different classical and generalized mechanical models are selected to identify a viscous device using experimental data. The main difference between classical and generalized models is that the generalized one incorporates a nonlinearity in spring and viscous elements; in addition, the resistant forces of generalized models have fractional exponential coefficients.

Linear viscous model

The simplest way to model a velocity dependent mechanical law is by means of the standard linear viscous model. The equation of the motion of a FVD modeled in this way and subject to a time-varying force p is:

$$m\ddot{y} + C\dot{y} = p \quad (1)$$

This basic model has the main advantage to be extremely simple, but sometimes it is too poor for a reasonable representation of real mechanical behavior. For this reason, it has been updated by the non-linear viscous model that depends on a fractional exponent of the velocity instead of a simple linear relationship. Generalized non-linear viscous model is described below:

Generalized viscous model

It is a two parameters model proposed by Constantinou [26], [27] whose law is:

$$m\ddot{y} + C \operatorname{sgn}(\dot{y}) |\dot{y}|^\alpha = p \quad (2)$$

where α is the damping term exponent, whose value lies between 0 and 1. Various mechanical behaviors are associated to different values of α . For instance, if $\alpha = 1$ the linear viscous damping law corresponds; if $\alpha = 0$ the dry friction appears (consequently, the force increases quickly for small velocity values, and becomes almost constant for large velocity values). This damping law has been widely adopted by various authors thanks to its ability in structural behavior modeling. For example, Lin and Chopra [28] make use of this constitutive law in the investigation of the earthquake induced response. In addition, this law is adopted in many structural computer codes.

However, experimental studies demonstrated that the resistance force of viscous dampers depends not only on damper velocity, but also on damper deformation. This mechanical property may be mathematically modeled connecting a spring element and a viscous element, respectively. If these two elements are connected in parallel, the family of Kelvin-Voigt models is obtained. For example, if a linear spring is connected in parallel with the simple linear dashpot, the basic Kelvin-Voigt

model is derived. When non-linear springs are connected with generalized non-linear viscous models, other behaviors are obtained. In [29] Terenzi investigated linear and parabolic models for the elastic force ψ_e :

$$\psi_e = K_1 y \quad (3)$$

$$\psi_e = K_2 y^2 + K_1 y + K_0 \quad (4)$$

where K_1 is the elastic stiffness, K_2 and K_0 are two constants. In [29], the authors stated that the parabolic function reproduces better the shape of the test cycles, but the linear function may be preferable, because it is simpler and yields a comparable energy balance.

Generalized viscous – linear elastic model

By combining Eq.(2) and Eq.(3), the equation of motion of a generalized Kelvin-Voigt model, subjected to a time-varying force p is derived:

$$m\ddot{y} + C \operatorname{sgn}(\dot{y}) |\dot{y}|^\alpha + K_1 y = p \quad (5)$$

Generalized viscous – quadratic elastic model

In this model, the parabolic form in Eq.(4) is considered without the constant K_0 :

$$m\ddot{y} + C \operatorname{sgn}(\dot{y}) |\dot{y}|^\alpha + K_1 y + K_2 y^2 = p \quad (6)$$

IDENTIFICATION: OPTIMIZATION PROBLEM

The second step of parameter identification requires the formalization of a suitable objective function to be minimized.

The model parameters \mathbf{x} of the viscous damper are identified by solving the following single-objective optimization problem:

$$\min_{\mathbf{x}} \{f(\mathbf{x})\}$$

s.t. $\mathbf{x}^l \leq \mathbf{x} \leq \mathbf{x}^u$

where $\mathbf{x} = \{x_1, \dots, x_j, \dots, x_n\}$ is a set of real parameters (in this case \mathbf{x} collects the mechanical model parameters), $\mathbf{x}^l = \{x_1^l, \dots, x_j^l, \dots, x_n^l\}$ and $\mathbf{x}^u = \{x_1^u, \dots, x_j^u, \dots, x_n^u\}$ are lower and upper bounds of \mathbf{x} , respectively. The solution that minimizes the objective function (OF) $f(\mathbf{x})$ is \mathbf{x}^* .

The following integral is assumed as measure to define the OF in the identification problem:

$$f(\mathbf{x}) = \frac{1}{\sigma_{p_m} (t_{end} - t_{start})} \int_{t_{start}}^{t_{end}} (p_m - p_e(\mathbf{x})) dt \quad (7)$$

where t_{start} and t_{end} are the start and end time records, $p_m(t)$ is the force measured, while $p_e(t)$ is the force estimated. This is obtained by numerical differentiation of experimental displacement time history with a 3rd order algorithm to limit numerical noise. One should point out that the evaluation of this OF is extremely computational cheap if compared with alternative approaches, in which the duality of starting from an experimental force leads to the theoretical displacement, obtained by integration as a solution of the differential equation. The optimization problem is solved by Particle Swarm Optimization (PSO).

Experimental studies

Test apparatus

The 750 kN viscous damper was tested at SISMALB srl laboratory in Taranto, Italy. The test setup (Figure 1) consists of a high resistance steel frame to withstand loads of tension and compression of 2200 KN. The device is anchored to the structure by means of a pin, and is stilled to the servant cylinder by means of a threaded connection. The movements are generated by a servant cylinder of 1400 KN, controlled in force and/or displacement. Between the servant cylinder and the device a load cell of 2500 KN is located, which acquires the forces applied to the device during the entire duration of the experiment. In a displacement imposed test, the device movements are controlled by a transducer mounted on the device. The control and data acquisition system is able to generate a real time analysis of device displacements, by instantaneously variation of applied forces by the servant cylinder by means of a computer automatic control hydraulic pressure system. The displacement time history can be imposed with different laws, from sinusoidal, triangular, or through a generator step of generic ones. This system is able to control applied forces in real time according to the imposed displacement or force imposed test. Acquiring system has 30 channels and can command 2 actuators at the same time.

Table 1 shows the design characteristics of the tested FVD.



Figure 1. View of the viscous test machine and fluid viscous damper

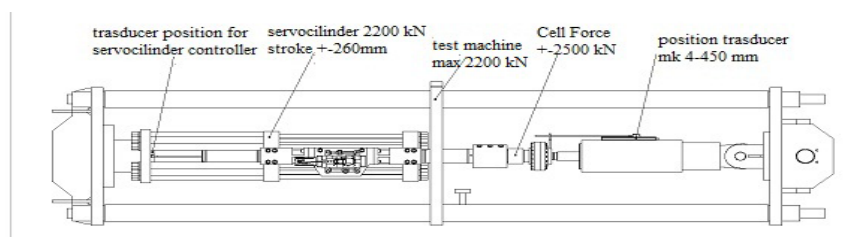


Figure 2. A photo of the test apparatus with the fluid viscous damper

Table 1 Fluid Viscous Damper Design Condition

F [kN]	Stroke [mm]	C [kN/(mm/s)]	V [mm/s]	α
750	± 100	406.24	460	0.1

Test cases

Four experiments were performed to obtain dynamic response of the viscous damper. The experiments were designed to determine the dynamic characteristics of the damper at varying velocities and to evaluate the effective energy dissipation of the device. The damper was subjected to multiple sets of monotonic sinusoidal excitations, at peak velocities of 92 mm/s, 230 mm/s, 460 mm/s (% refers to design velocity 460 mm/s) The first three tests have a 3-cycle excitation period, while the fourth test (energy dissipation test) has a 10-cycle period. The test specifications are summarized in Table 2.

Table 2. Fluid viscous damper test condition

No.	Test Type	Load (kN)	Test stroke (±mm)	Velocity (mm/s)	Cycle
1	Constitutive law test	750	20	92 (20%)	3
2		750	20	230 (50%)	3
3		750	20	460 (100%)	3
4	Damping efficiency test	750	17	460 (100%)	10

Parametric identification

For the evaluation of optimal values of the unknown parameters in Equations (1), (2), (5), (6) the parametric identification performed by PSO, was applied with a population size N=50 and maximum number of iterations L=100. The parametric identification has been performed by solving the single-objective optimization problem, whose objective function is given by Equation (7). The algorithms have been performed fifty times, and the best solution has been carried out as the final identification result.

Identification results

This subsection shows the identified parameter values that best fit the test results for the four analyzed models. Table 3, Table 4, Table 5 and Table 6 show the best (Min), worst (Max), mean and standard deviation (Std) values of the OF obtained under different numerical tests, for the four analyzed models. Data are represented also in Figure 3.

Table 3. Objective Function results obtained from the PSOA using the linear viscous mechanical model for four different experimental tests

Mechanical Model: <i>Linear viscous</i>				
Test	Mean	Max	Min	Std
Test 1	0.324322	0.324322	0.324322	0
Test 2	0.363997	0.363997	0.363997	2.8E-16
Test 3	0.272685	0.272685	0.272685	1.68E-16
Test 4	0.297829	0.297829	0.297829	1.68E-16

Table 4 Objective Function results obtained from the PSOA using the Generalized viscous mechanical model for four different experimental tests

Mechanical Model: <i>Generalized viscous</i>				
Test	Mean	Max	Min	Std
Test 1	0.254494	0.254494	0.254494	4.26E-14
Test 2	0.332256	0.332257	0.332256	1.39E-07
Test 3	0.264244	0.26426	0.264243	2.99E-06
Test 4	0.28234	0.28234	0.28234	2.45E-09

Table 5 Objective Function results obtained from the PSOA using the Generalized viscous – linear elastic mechanical model for four different experimental tests

Mechanical Model: <i>Generalized viscous- linear elastic</i>				
Test	Mean	Max	Min	Std
Test 1	0.162356	0.163188	0.162077	0.000298
Test 2	0.203976	0.204116	0.203949	3.45E-05
Test 3	0.153384	0.153388	0.153384	7.23E-07
Test 4	0.127699	0.127699	0.127699	1.41E-12

Table 6. Objective Function results obtained from the PSOA using the Generalized viscous – quadratic elastic mechanical model for four different experimental tests

Mechanical Model: <i>Generalized viscous- quadratic elastic</i>				
Test	Mean	Max	Min	Std
Test 1	0.173636	0.254494	0.158448	0.022962
Test 2	0.208454	0.21712	0.203949	0.006284
Test 3	0.160706	0.26426	0.153025	0.026845
Test 4	0.12752	0.127699	0.126207	0.00049

Tables 7-10 show the values of identified parameters obtained for each mechanical model, where mean, max, min and std indicate the values which correspond to mean, max, min and std of OF in previous tables. Results of identification are represented also in Figures 4-7.

Table 7. Values of mechanical parameters obtained in four different test types, using the linear viscous mechanical model of FVD

Mechanical Model: <i>Linear viscous</i>				
Parameters	Test Type N.1	Test Type N.2	Test Type N.3	Test Type N.4
	v=92mm/s	v=230mm/s	v=460mm/s	v=460mm/s
M(mean) - [kg]	0	0	0	0
M(max) - [kg]	0	0	0	0
M(min) - [kg]	0	0	0	0
C(mean) - [kN/(mm/s)]	6.308518	9.955068	2.950677	3.599261
C(max) - [kN/(mm/s)]	6.308518234	9.955068455	2.95067697	3.599260974
C(min) - [kN/(mm/s)]	6.308518234	9.955068455	2.95067697	3.599260974
C(std)-[kN/(mm/s)]	3.32E-14	0	1.93E-15	3.15E-14

Table 8. Values of mechanical parameters obtained in four different test types, using the fractional viscous mechanical model of FVD

Mechanical Model: <i>Fractional viscous</i>				
Parameters	Test Type N.1	Test Type N.2	Test Type N.3	Test Type N.4
	v=92mm/s	v=230mm/s	v=460mm/s	v=460mm/s
M(mean) - [kg]	1.75E-14	1.45E-11	0	0
M(max) - [kg]	8.74059E-13	7.26404E-10	0	0
M(min) - [kg]	0	0	0	0
M(std) - [kg]	1.24E-13	1.03E-10	0	0
C(mean) - [kN/(mm/s) ^ α]	321.4664	101.8108	20.93332	60.02495
C(max) - [kN/(mm/s) ^ α]	321.4663828	102.5398101	22.44238445	60.02544199
C(min) - [kN/(mm/s) ^ α]	321.4663828	101.058709	20.75427774	60.01439848
C(std) - [kN/(mm/s) ^ α]	1.05E-10	0.254748	0.284589	0.001661
α (mean)	0.121515	0.456479	0.647184	0.472998
α (max)	0.121514934	0.458176548	0.648755563	0.473033897
α (min)	0.121514934	0.454813372	0.634798957	0.472996579
α (std)	6.82E-14	0.00058	0.002352	5.61E-06

Table 9. Values of mechanical parameters obtained in four different test types, using the fractional viscous –linear elastic mechanical model of FVD

Mechanical Model: Fractional viscous- linear elastic				
Parameters	Test Type N.1	Test Type N.2	Test Type N.3	Test Type N.4
	v=92mm/s	v=230mm/s	v=460mm/s	v=460mm/s
M(mean) - [kg]	2.034798	1.820115	0.000221	4.88E-12
M(max) - [kg]	2.198171813	1.904731018	0.004116766	2.43898E-10
M(min) - [kg]	1.810732517	1.602184231	0	0
M(std) - [kg]	0.089231	0.077191	0.000761	3.45E-11
C(mean) - [kN/(mm/s) ^ α]	52.61233	24.70355	2.924908	3.575181
C(max) - [kN/(mm/s) ^ α]	58.98786914	24.94752828	2.925077333	3.575181353
C(min) - [kN/(mm/s) ^ α]	48.52647178	24.41265785	2.924898421	3.575181353
C(std) - [kN/(mm/s) ^ α]	3.512028	0.125295	3.31E-05	8.73E-11
α (mean)	0.510677	0.768888	1	1
α (max)	0.52834009	0.772247572	1	1
α (min)	0.484805623	0.766278406	1	1
α (std)	0.014462	0.001346	0	0
K_0 (mean) - [kN/mm]	70.59402	41.37259	9.3253	13.89884
K_0 (max) - [kN/mm]	75.50983233	42.59740601	10.00317587	13.89884259
K_0 (min) - [kN/mm]	63.74648345	38.15868057	9.286881568	13.89884253
K_0 (std) - [kN/mm]	2.749654	1.129993	0.132487	9.43E-09

Table 10. Values of mechanical parameters obtained in four different test types, using the fractional viscous – quadratic elastic mechanical model of FVD

Mechanical Model: Fractional viscous- quadratic elastic				
Parameters	Test Type N.1	Test Type N.2	Test Type N.3	Test Type N.4
	v=92mm/s	v=230mm/s	v=460mm/s	v=460mm/s
M(mean) - [kg]	1.528561	1.22022	0.007768	1.00E-15
M(max) - [kg]	2.180005282	1.921826379	0.189771629	4.99811E-14
M(min) - [kg]	0	0	0	0
M(std) - [kg]	0.861915	0.886947	0.032415	7.07E-15
C(mean) - [kN/(mm/s) ^ α]	67.00402	25.31663	4.324775	3.574265
C(max) - [kN/(mm/s) ^ α]	321.4663828	26.52458809	22.43076879	3.57518146
C(min) - [kN/(mm/s) ^ α]	48.53968825	24.39242143	2.924898421	3.567545202
C(std) - [kN/(mm/s) ^ α]	52.75564	0.696476	4.821501	0.002507
α (mean)	0.480449	0.764121	0.972133	1
α (max)	0.527975613	0.771759295	1	1
α (min)	0.121514934	0.753137579	0.634903225	0.999999994
α (std)	0.077104	0.005187	0.095558	7.80E-10
K ₁ (mean) - [kN/mm]	55.07667	32.25728	10.0696	13.94087
K ₁ (max) - [kN/mm]	74.9994301	42.88675282	42.85875522	14.24910384
K ₁ (min) - [kN/mm]	0	13.76515596	0	13.89884243
K ₁ (std) - [kN/mm]	26.29288	13.44016	6.269791	0.114977
K ₂ (mean) - [kN/mm ²]	0.007748	0	0.002121	0.010372
K ₂ (max) - [kN/mm ²]	0.082770673	0	0.036533794	0.086436416
K ₂ (min) - [kN/mm ²]	0	0	0	0
K ₂ (std) - [kN/mm ²]	0.023509	0	0.008492	0.028374

COMPARISON OF HYSTERESIS LOOPS PREDICTED BY VARIOUS MODELS

In figures 3-6 the experimental hysteresis loops of the damper under investigation are compared with those simulated by the selected models previous described, for load application velocities V_1 , V_2 , V_3 and V_4 . More precisely, in figures 3 and 4, the relationships between displacement and forces are shown, whereas figures 5 and 6 illustrate the relationships between force and velocity. The dotted lines represent the experimental loops, while the solid lines are the theoretical loops obtained by using the identified parameters for each assessed model.

From these plots one can notice that the experimental and theoretical loops have exactly the same relative displacement (and velocity), whereas the damper force of the theoretical loop is computed according to each model. The experiment loops in Figures 3 and 4 show that, under harmonic excitation, the hysteresis loop of the damper changes when load application velocity increases. The comparison between theoretical and simulated loops points out that the simulated results obtained by the *generalized viscous – linear elastic* model ((b) in figure 3) match well with the experimental loops under all the excitation frequencies. The agreement of this model with experimental loop is better with respect to the *linear viscous elastic one* ((a) in figure 3). On the other hand, the other

analyzed models lead to elliptic hysteresis loops. For this reason, these cannot match well with the experimental loops for all the frequencies, because the loop changes its shape from low to high frequencies. For example, the *linear viscous model* underestimates the force for all frequencies and especially at low frequency.

With reference to *generalized viscous – linear elastic* ((c) in figure 4) and *generalized viscous – quadratic elastic* ((d) in figure 4) models, one can observe a good match with experimental loops for all velocities of the load application. The third and the fourth models predict well the force; in effect, one should consider another aspect, i.e. the area of the loop, which represents the amount of dissipated energy in the cycle. The plots point out that the *generalized viscous – linear elastic* model overestimates the amount of dissipated energy for all velocities of load application. On the contrary, the *generalized viscous – quadratic elastic* predicts fine the dissipated energy, especially for high load application velocity. The same observation can be pointed out with reference to *generalized viscous – quadratic elastic* model.

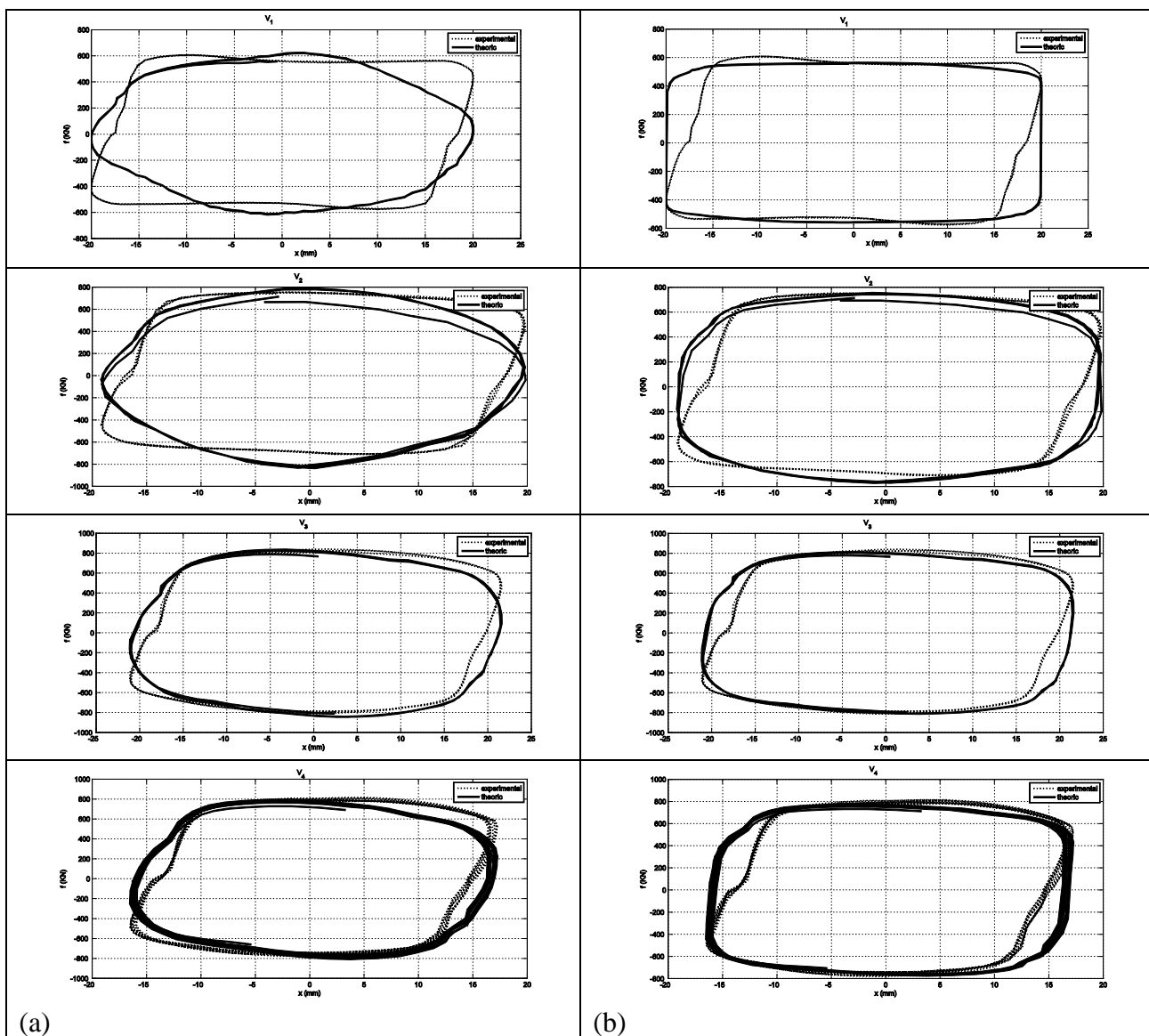


Figure 3. Comparison between theoretical and experimental force- displacement relationship: a) Linear viscous model, b) Generalized viscous model.

In figures 5 and 6 the relationships between the force and the velocity are shown. The first and the second model don't predict absolutely the experimental force -velocity experimental loop, whereas the third and the fourth model match satisfactorily the experimental loop, especially for high excitation frequency.

Because the matching of the identified model with the experimental ones depends on the excitation frequency, it is interesting to evaluate the sensitivity of identified parameters against the frequency excitation. For this purpose, for each model, the mean value \bar{p} of each identified parameter p , evaluated from the four tests is extrapolated; the range of variation $\Delta\bar{p} = \bar{p}_{\max} - \bar{p}_{\min}$ and the ratio $\Delta\bar{p} / \bar{p}$ are furnished (table 11-14) to quantify the variability of mentioned parameters with respect to the test conditions. From numerical data in tables 11-14, one can deduce that, except for the *linear viscous model*, the parameter C exhibits the highest variability against the velocity of the external excitation application. Anyway, all analyzed models present almost a comparable variability of involved parameters.

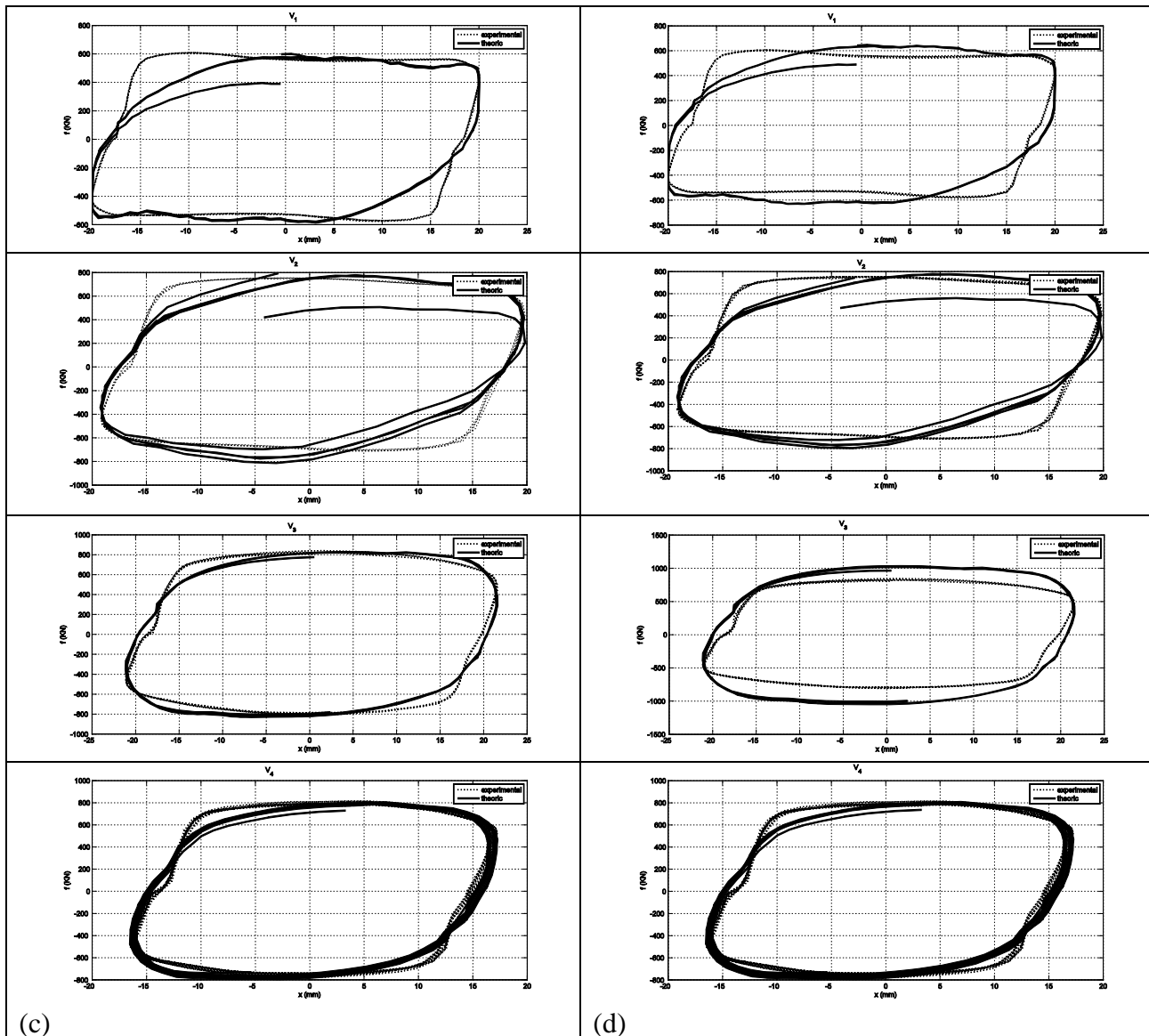


Figure 4. Comparison between theoretical and experimental force- displacement relationship:
c) Generalized viscous- linear elastic, d) Generalized viscous- quadratic elastic.

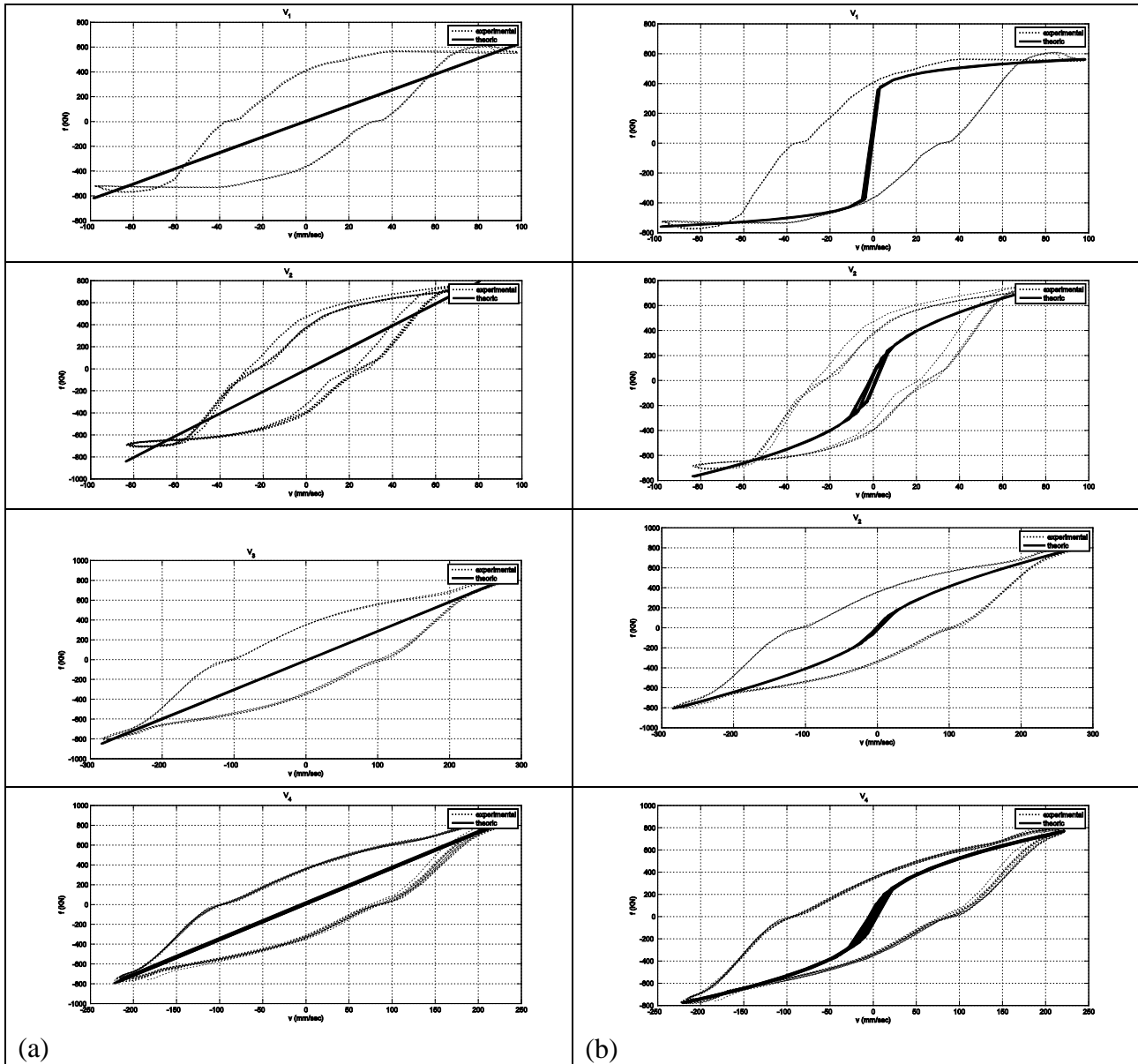


Figure 5. Comparison between theoretical and experimental force- velocity relationship: a) Linear viscous model, b) Generalized viscous model.

Table 11. Parameters sensitivity of Linear viscous mechanical model

\bar{M} [kg]	0
$\Delta\bar{M}$	0
$\Delta\bar{M} / \bar{M}$	0
\bar{C} [kN/(mm/s)]	5,703381
$\Delta\bar{C}$	7,004391
$\Delta\bar{C} / \bar{C}$	1,228112

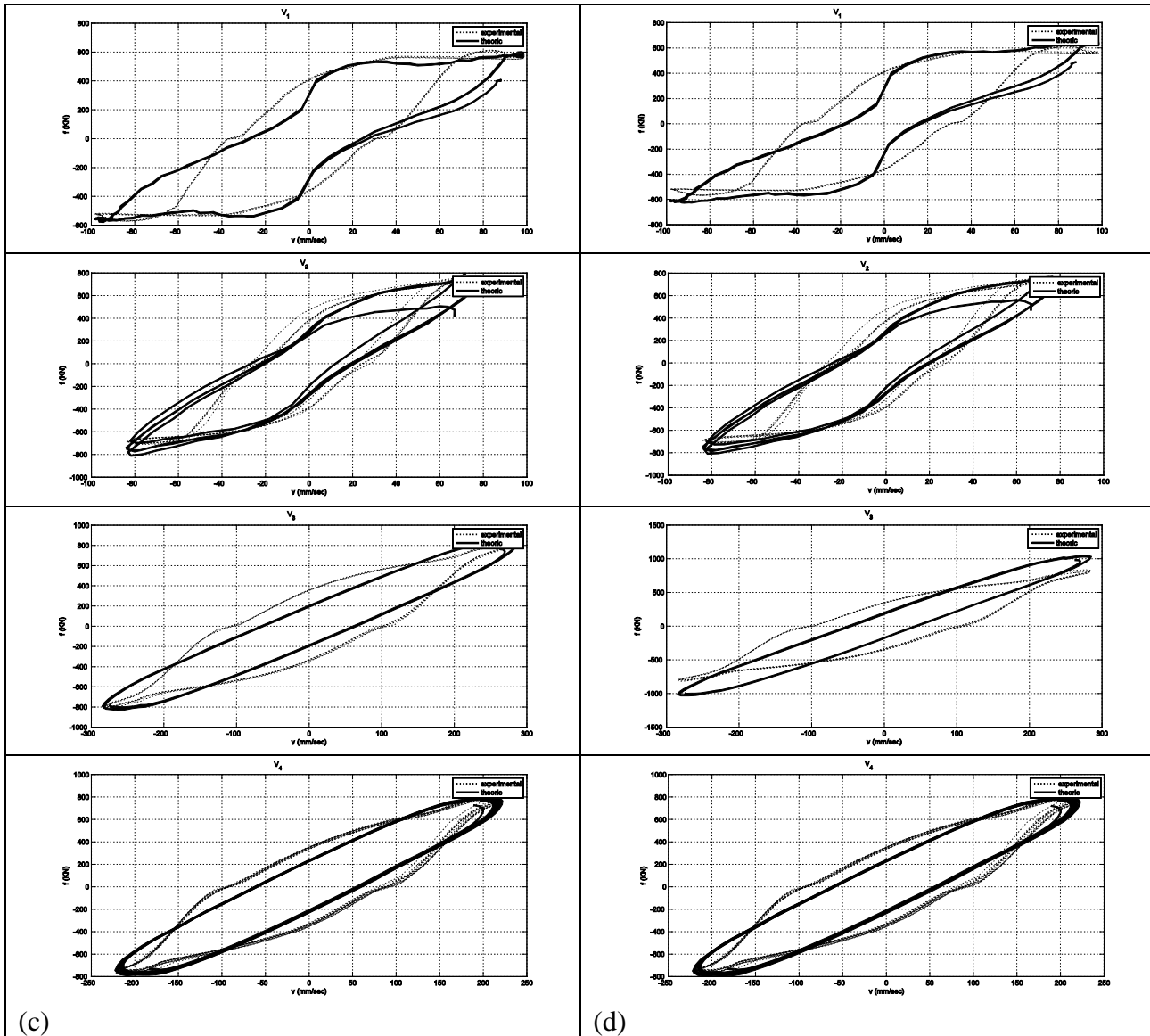


Figure 6. Comparison between theoretical and experimental force- velocity relationship: c) Generalized viscous- linear elastic, d) Generalized viscous- quadratic elastic.

Table 12. Parameters sensitivity of generalized viscous mechanical model

\bar{C} - [kN/(mm/s) $^{\alpha}$]	126,0589
$\Delta\bar{C}$	300,5331
$\Delta\bar{C} / \bar{C}$	2,384069
$\bar{\alpha}$	0,424544
$\Delta\bar{\alpha}$	0,525669
$\Delta\bar{\alpha} / \bar{\alpha}$	1,238197

Table 13: Parameters sensitivity of Generalized viscous- linear elastic mechanical model

\bar{M} [kg]	0,963784
$\Delta\bar{M}$	2,03E+00
$\Delta\bar{M} / \bar{M}$	2,11E+00
\bar{C} [kN/(mm/s) ^{α}]	20,95399
$\Delta\bar{C}$	49,68742
$\Delta\bar{C} / \bar{C}$	2,371263
$\bar{\alpha}$	0,819891
$\Delta\bar{\alpha}$	0,489323
$\Delta\bar{\alpha} / \bar{\alpha}$	0,596815
\bar{K}_0 - [kN/mm]	33,79769
$\Delta\bar{K}_0$	61,26872
$\Delta\bar{K}_0 / \bar{K}_0$	1,812808

Table 14: Parameters sensitivity of Generalized viscous- quadratic elastic mechanical model

\bar{M} [kg]	0,689137
$\Delta\bar{M}$	1,53E+00
$\Delta\bar{M} / \bar{M}$	2,22E+00
\bar{C} [kN/(mm/s) ^{α}]	25,05492
$\Delta\bar{C}$	63,42976
$\Delta\bar{C} / \bar{C}$	2,531628
$\bar{\alpha}$	0,804176
$\Delta\bar{\alpha}$	0,519551
$\Delta\bar{\alpha} / \bar{\alpha}$	0,646066
\bar{K}_1 - [kN/mm]	27,83611
$\Delta\bar{K}_1$	45,00707
$\Delta\bar{K}_1 / \bar{K}_1$	1,616859
\bar{K}_2 - [kN/mm ²]	0,00506
$\Delta\bar{K}_2$	0,010372
$\Delta\bar{K}_2 / \bar{K}_2$	2,049701

Conclusions

This study concentrates on classical and generalized mechanical models for FVD. The focal difference between classical and generalized models is that the generalized ones incorporate nonlinearity in spring and viscous elements; in addition, the resistant forces in generalized models have fractional exponential coefficients. To evaluate the effectiveness of diverse models to catch the hysteretic behavior of real FVDs, diverse analytical models have been identified on the basis of experimental tests. The identification procedure is performed comparing the experimental and the analytical values of the forces experienced by the device under investigation. The experimental forces have been recorded during the dynamic test and the analytical ones have been evaluated by imposing the time history of displacement to the candidate mechanical law. The parametric identification of a real FVD has been developed by Particle Swarm Optimization. The identification process furnishes the best mechanical parameters by minimizing the difference between analytical and experimental applied forces. Four experiments have been performed to obtain the dynamic response of the viscous damper under investigation, varying the velocity of the load application. The results show that the analytical results obtained by the generalized viscous – linear elastic model match well the experimental loops, under all the excitation frequencies, better with respect the linear viscous elastic one. Moreover, with reference to generalized viscous – linear elastic and generalized viscous – quadratic elastic it has been observed a good match with experimental loops for all velocities of the load application. The generalized viscous – linear elastic model and the generalized viscous – quadratic elastic model one predict well the force, but the generalized viscous – linear elastic overestimates the amount of dissipated energy for all velocities of the load application. On the contrary, the generalized viscous – quadratic elastic predicts well the energy dissipated, especially for high velocity of load application. The same observation can be made with reference to generalized viscous – quadratic elastic model. Moreover, the sensitivity of identified parameters against the frequency excitation has been investigated. Results showed that, except for the linear viscous model, the parameter C exhibits the highest variability against the velocity of the external excitation application. Anyway, all analyzed models present almost a comparable variability of involved parameters.

Acknowledgement

This work is framed within the research project\DPC-243 ReLUIIS 2014, RS4 “Monitoraggio” and RS11 "Trattamento delle incertezze nella valutazione degli edifice esistenti".

References

- [1] Soong TT, Dargush GF (1997) Passive energy dissipation systems in structural engineering. John Wiley & Sons, New York.
- [2] Marano GC, Trentadue F, Greco R (2007) Stochastic optimum design criterion for linear damper devices for seismic protection of buildings. *Structural and Multidisciplinary Optimization* 33:441-455
- [3] Marano GC, Trentadue F, Greco R (2007) Stochastic optimum design criterion of added viscous dampers for buildings seismic protection. *Structural Engineering and Mechanics* 25(1): 21-37
- [4] Yun HB, Tasbighoo F, Masri SF, Caffrey JP, Wolfe RW, Makris N, Black C (2008) Comparison of Modeling Approaches for Full-scale Nonlinear Viscous Dampers. *Journal of Vibration and Control* 14:51-76
- [5] Constantinou MC and Symans MD (1993) Experimental study of seismic response of buildings with supplemental fluid dampers. *Structural Design of Tall Buildings* 2:93–132
- [6] Schurter KC, Roschke PN (2000) Fuzzy modeling of a magnetorheological damper using ANFIS. *Proceedings of the Ninth IEEE International Conference on Fuzzy Systems*, San Antonio, TX, 122–127.
- [7] Wang DH, Liao WH (2001) Neural network modeling and controllers for magnetorheological fluid dampers. *Proceedings of the 2001 IEEE International Conference on Fuzzy Systems*, Melbourne, Australia, 1323–1326.
- [8] Man KF, Tang KS, Kwong S (1996) Genetic algorithms: concepts and applications. *IEEE Trans. Ind. Electron* 43:519–534
- [9] Goldberg DE (1989) *Genetic Algorithms in Search, Optimization and Machine Learning*. Addison-Wesley, Reading, MA
- [10] Iwasaki M, Miwa M, Matsui N (2005), GA-based evolutionary identification algorithm for unknown structured mechatronic systems. *IEEE Trans. Ind. Electron* 52: 300–305.

- [11] Ha JL, Kung YS, Fung RF, Hsien SC (2006) A comparison of fitness functions for the identification of a piezoelectric hysteretic actuator based on the real-coded genetic algorithm. *Sensors and Actuators A* 132:643-650
- [12] Kwok NM, Ha QP, Nguyen MT, Li J, Samali B (2007) Bouc-Wen model parameter identification for a MR fluid damper using computationally efficient GA. *ISA Transactions* 46:167-179
- [13] Hornig KH, Flowers GT (2005) Parameter characterization of the Bouc-Wen mechanical hysteresis model for sandwich composite materials using real coded genetic algorithms. *The International Journal of Acoustics and Vibration* 10(2):73-81
- [14] Ajavakom N, Ng CH, Ma F (2008) Performance of nonlinear degrading structures: identification, validation, and prediction. *Computer and Structure* 86:652-662
- [15] Giuclea M, Sireteanu T, Stancioiu D, Stammers CW (2004a) Modelling of magnetorheological damper dynamic behavior by genetic algorithms based inverse method. *Proceedings of the Romanian Academy Series A* 5(1):55-63
- [16] Giuclea M, Sireteanu T, Stancioiu D, Stammers CW, (2004b) Model parameter identification for vehicle vibration control with magnetorheological dampers using computational intelligence methods. *Proceedings of the institution of mechanical engineers. Part I: Journal of Systems and Control Engineering* 218(7):569-581
- [17] Kwok NM, Ha QP, Nguyen MT, Li J, Samali B (2007) Bouc-Wen model parameter identification for a MR fluid damper using computationally efficient GA. *ISA Transactions*, 46(2):167-179
- [18] Charalampakis AE, Koumousis VK (2008) Identification of Bouc-Wen hysteretic systems by a hybrid evolutionary algorithm. *Journal of Sound and Vibration* 314:571-585
- [19] Sireteanu T, Giuclea M, Mitu AM (2010) Identification of an extended Bouc-Wen model with application to seismic protection through hysteretic devices. *Computational Mechanics* 45(5):431-441
- [20] Kennedy J, and Eberhart R C (1995) Particle Swarm Optimization. *Proceedings of IEEE International Conference on Neural Networks*, Perth, Australia 1942-1948
- [21] Gaing ZL (2004) A particle swarm optimization approach for optimum design of PID controller. AVR system, *IEEE Trans. Energy Conversion* 19:384-391
- [22] Ciuprina G, Loan D, Munteanu I (2002) Use of intelligent-particle swarm optimization in electromagnetics. *IEEE Trans. Magn.* 38:1037-1040
- [23] Trelea IC (2003). The particle swarm optimization algorithm: convergence analysis and parameter selection. *Inf. Process. Lett.* 85:317-325.
- [24] Kwok MN, Ha QP, Nguyen TH, Li J, Samali B (2006) A novel hysteretic model for magnetorheological fluid dampers and parameter identification using particle swarm optimization. *Sensors and Actuators A* 132: 441-451
- [25] Greco R, Marano GC (2013) Identification of parameters of Maxwell and Kelvin-Voigt generalized models for fluid viscous dampers. *Journal of Vibration and Control* doi: 10.1177/1077546313487937.
- [26] Constantinou MC and Symans MD (1993) Experimental study of seismic response of buildings with supplemental fluid dampers. *Structural Design of Tall Buildings* 2:93-132
- [27] Constantinou MC, Symans MD, Tsopelas P, Taylor DP (1993), Fluid viscous dampers in applications of seismic energy dissipation and seismic isolation. in *Proceedings of ATC 17-1 Seminar on Seismic Isolation, Passive Energy Dissipation and Active Control V.* 2:581-592
- [28] Lin WH, Chopra AK (2003) Asymmetric One-Storey Elastic Systems with Non-linear Viscous and Viscoelastic Dampers. *Earthquake Response, Earthquake Engineering and Structural Dynamics* 32:555-577
- [29] Terenzi G (1999) Dynamics of SDOF Systems with Nonlinear Viscous Damping. *Journal of Engineering Mechanics* 125:956-963
- [30] Sh, Y, Eberhart R (1998) A modified particle swarm optimizer. *IEEE World Congress on Computational Intelligence*, Anchorage, AK, USA, May 4-9
- [31] Ratnaweera A, Halgamuge SK, Watson HC (2004) Self-Organizing Hierarchical Particle Swarm Optimizer With Time-Varying Acceleration Coefficients. *IEEE Transactions on Evolutionary Computation* 8:240-255